E-ISSN: 111 – 2716 P-ISSN: 3026 – 8214
MPRI-JAAER | INTERNATIONAL JOURNAL OF APPLIED & ADVANCED ENGINEERING RES.
VOL. 14 NO. 5 OCTOBER, 2026

COMPARATIVE ASSESSMENT OF HYBRID STORAGE CONFIGURATIONS FOR VOLTAGE AND FREQUENCY SUPPORT IN AN ISLANDED RENEWABLE MICROGRID

KENNETH UGO UDEZE; KENECHI MARKANTHONY ONWUGHALU; & MEZUE FRANCIS CANICE TOCHUKWU

Department of Electrical & Electronics Engineering, Federal Polytechnic Oko, Anambra State, Nigeria.

DOI: https://doi.org/10.70382/mejaaer.v14i5.070

Abstract

The increasing integration of renewable energy sources into islanded microgrids introduces operational challenges associated with power variability, limited conventional rotational inertia, and the need for effective energy storage management. Hybrid energy storage systems (HESS) provide a potential approach to addressing these challenges by combining technologies with complementary power and energy characteristics. This paper presents a comparative evaluation of five energy storage and control configurations in an islanded photovoltaic–wind–diesel microgrid comprising a 17 kW photovoltaic system, a 48 kW wind turbine, and a 100 kW diesel generator. The configurations investigated include a battery energy storage system (BESS) operating alone, BESS integrated with superconducting magnetic energy storage (SMES) under constant and dynamic droop control, and a combined BESS–SMES–supercapacitor (SC) system under both control strategies. Particular attention is given to the reported state-of-charge (SOC) operating ranges and total harmonic distortion (THD) results. The BESS-only configuration exhibits an SOC range of 5–92%, corresponding to a range width of 87 percentage points. In comparison, the BESS–SMES–SC configuration employing enhanced dynamic droop control operates within a reported SOC range of 48–74%, giving a range width of 26 percentage points. This represents a 61-percentage-point reduction in SOC-range width relative to the BESS-only

Keywords: Islanded microgrid; hybrid energy storage system; state of charge; battery energy storage system; superconducting magnetic energy storage; supercapacitor; dynamic droop control; photovoltaic–wind–diesel system.

EDITOR-IN-CHIEF
Prof. Saeid Eslamian [IRAN]

configuration. The results suggest that combining complementary storage technologies with dynamic droop control can provide more constrained SOC operation within the configurations examined. The comparative analysis offers a basis for evaluating storage-system selection and control strategies in islanded renewable microgrids. Further validation of harmonic measurements and quantitative voltage and frequency responses is required to establish the broader power-quality and dynamic-stability implications of the findings.

Introduction

High penetration of converter-interfaced renewable generation can make islanded microgrids more sensitive to power imbalance, particularly when conventional synchronous generation is displaced and the available inertial response is reduced. In a stand-alone system, load changes and renewable-output fluctuations can produce frequency deviations and voltage excursions because the main grid is not available to absorb the imbalance. Microgrid control research has therefore considered primary droop control, hierarchical control, storage-based frequency support, and coordinated operation of distributed energy resources [1]–[5].

A battery energy storage system can provide substantial energy capacity, but frequent high-rate charge/discharge cycles may accelerate degradation. Reviews of electrical storage and microgrid HESS applications emphasize that combining devices with different energy and power characteristics can improve dynamic response, although performance depends on topology, control design, converter interfaces, and sizing [6]–[8]. Battery–supercapacitor systems have been studied for fast power support and battery stress reduction [9], [10], while SMES–battery arrangements have been examined for primary frequency control and battery-lifetime considerations [11], [12]. The project considered a three-technology arrangement adding a supercapacitor and an enhanced dynamic droop controller, with the objective of coordinating storage responses and limiting battery SOC excursions.

The objectives are to model a multi-source islanded microgrid, implement its mathematical models in MATLAB/Simulink, assess the Secant-based dynamic droop controller described in the project report, and compare reported primary-frequency-control, voltage-regulation, battery-SOC, and THD outcomes across storage configurations. The contribution claimed here is limited to the comparative assessment documented in the source report; controller novelty and implementation details should be verified against the original MATLAB code and prior publications before submission.

The literature indicates three relevant design considerations. First, droop-based control is widely used for decentralized sharing but involves trade-offs among stability, voltage/frequency deviation, and power sharing [1], [2], [13], [14]. Second, storage technologies have complementary dynamic characteristics: batteries provide energy capacity, while supercapacitors and SMES can respond rapidly to short-duration fluctuations [6], [8], [15]. Third, a HESS control strategy should be assessed not only by transient voltage and frequency behaviour but also by SOC constraints,

EDITOR-IN-CHIEF
Prof. Saeid Eslamian [IRAN]

converter limits, and transparent power-quality metrics [11], [12], [16]. The present source report does not provide enough numerical time-series data to quantify several of these metrics independently, so these issues are treated as validation priorities rather than assumed benefits. Prior work has also addressed optimal battery sizing for islanded-microgrid frequency control, storage-based frequency support, and coordinated battery control in microgrids [17]–[19]. Studies of wind-power participation and reduced rotational inertia further motivate fast-response support in islanded systems [20], [21]. For the hybrid renewable supply context, remote-island PV–wind–battery feasibility studies provide a useful system-level comparison [22]. Finally, harmonic results should be assessed against an explicit measurement method and applicable limits or recommended practices, rather than inferred from relative reductions alone [23], [24].

Control context and research gap

Microgrid control is commonly organised into primary, secondary, and tertiary layers. Primary control responds locally and rapidly to electrical deviations; secondary control restores frequency and voltage deviations introduced by primary droop; tertiary control addresses scheduling and power exchange over slower time horizons [2], [26]. This hierarchy is important when interpreting a storage controller: a primary droop law may improve immediate sharing, but it does not automatically guarantee zero steady-state error, optimal dispatch, or seamless transitions between operating modes. A paper should therefore identify which control layer is implemented and which performance objective is being tested.

Conventional droop control relates active-power deviation to frequency deviation and reactive-power deviation to voltage deviation. Its decentralized nature is useful where communication is limited, but the selected slopes influence the balance between power sharing and regulation accuracy. In resistive low-voltage networks, the simple separation between active-power/frequency and reactive-power/voltage channels can be weakened by network impedance, converter dynamics, and coupling between the axes. Reviews of droop methods consequently distinguish conventional, adaptive, virtual-impedance, and hierarchical approaches rather than treating them as interchangeable [13], [14], [26], [27].

The literature also shows that storage control cannot be evaluated independently of the storage technology. Batteries have comparatively high energy capacity but can be stressed by rapid and repeated power reversals. Supercapacitors can deliver and absorb high power over short intervals, although their energy capacity is limited. SMES can provide very fast response, but its practical deployment depends on superconducting equipment, cryogenic requirements, power conversion, protection, and cost. These characteristics motivate coordinated control, but the presence of additional devices does not by itself prove better performance: the controller must allocate power appropriately, respect device constraints, and avoid shifting stress to a different component [6]–[12], [15], [16].

Recent reviews of inverter-based and islanded microgrid control reinforce that frequency and voltage stability depend on the network, inverter-control structure, communication assumptions, and operating mode. They also identify the need for stronger comparative evaluation and reproducible controller descriptions [27], [28]. In this manuscript, these reviews are used to position the work, not to imply that the current simulation has been independently validated. The

EDITOR-IN-CHIEF
Prof. Saeid Eslamian [IRAN]

evidence available from the source project supports a comparison of reported SOC ranges and reported THD values, while numerical claims about frequency nadir, voltage deviation, settling time, and battery ageing remain outside the demonstrated evidence.

The specific gap addressed here is consequently narrow and evidence-led: to organise the source project's reported results across five storage/control combinations and examine what those results can and cannot establish about SOC management and power quality. This is not framed as proof that the Secant-based controller is universally superior, nor as a claim of a new control law without code-level comparison to prior dynamic-droop work. The earlier SMES–battery dynamic-droop study is especially relevant because it uses a related application and method [12]. Any final submission should explicitly disclose the relationship between this manuscript, the 2023 M.Sc. project, and the authors' 2024 journal publication, and should follow the target journal's rules for reuse and duplicate publication.

Scope and research questions

The assessment is guided by four questions. (1) How do the reported battery SOC endpoints vary as SMES and a supercapacitor are added to the storage arrangement? (2) What additional difference is reported when constant droop gain is replaced by dynamic droop gain for the same nominal storage combination? (3) Do the reported THD values follow the same ordering as the SOC ranges, and are their absolute magnitudes sufficiently documented to support a power-quality conclusion? (4) What data and controller details are needed before voltage and frequency improvements can be quantified independently? These questions deliberately separate source-reported observations from interpretations and from validation work still required.

System configuration and methodology

The simulated microgrid combines a PV array, wind turbine, and diesel generator with an AC microgrid bus. The reported ratings are 17 kW for PV, 48 kW for wind, and 100 kW for the diesel generator. Hybrid renewable microgrids combining PV, wind, diesel generation, and storage have been studied for remote and islanded applications [22], [25]. The storage/control comparison is related to earlier SMES–battery dynamic-droop research for an isolated microgrid [12]. The HESS is connected through power-electronic conversion interfaces and comprises BESS, SMES, and a supercapacitor. The nominal operating values used in the controller are 50 Hz and 400 V.

Power-balance interpretation

At the AC bus, the instantaneous active-power balance can be represented conceptually as Equ.1

$$P_{Load} + P_{Loss} = P_{PV} + P_{WT} + P_{DG} + P_{HESS} \quad (1)$$

Where P_{HESS} is positive when the storage system injects power and negative when it absorbs power. A mismatch between generation and demand produces a transient imbalance that must be managed by controllable generation, storage, and load response. This balance is a physical interpretation of the system architecture; the source extract does not supply the complete

EDITOR-IN-CHIEF
Prof. Saeid Eslamian [IRAN]

numerical dispatch schedule, load profile, or time-varying renewable profiles required to reconstruct the simulation.

For frequency support, storage can respond to deviations in frequency or frequency rate of change, while voltage support depends on reactive-power control, inverter limits, network impedance, and the controller's voltage reference. These services should not be conflated: active-power injection primarily supports the active-power balance and frequency, whereas reactive-power injection or absorption primarily affects voltage magnitude in many AC operating conditions. In weak or low-voltage networks, the coupling between active and reactive power can be significant. The original model's converter topology and control equations are therefore needed to establish exactly how the two channels were coordinated.

Storage complementarity and constraints

A hybrid energy storage system is usually motivated by the mismatch between energy capacity and response speed. A battery can sustain a power contribution over a comparatively long interval, but its current, SOC, temperature, and cycling history constrain permissible operation. A supercapacitor is better suited to short power pulses and rapid fluctuations, but its usable energy window may be much smaller. SMES can exchange power rapidly through its converter, while the coil current and stored magnetic energy remain subject to operating and protection limits. A coordinated controller should therefore assign power according to both the disturbance time scale and each device's feasible operating region.

A generic SOC update for a battery can be expressed as Equ.2

$$SOC_{k+1} = SOC_k + \frac{\eta_{ch} P_{ch}(\mathrm{k})\Delta t}{E_{nom}} - \frac{P_{dis}(k)\Delta t}{\eta_{dis} E_{nom}} \qquad (2)$$

where SOC(k) and SOC(k+1) denote the battery's SOC at consecutive sampling instants; $P_{ch}(k)$ and $P_{dis}(k)$ are nonnegative charging and discharging powers, η_{ch} and η_{dis} are the corresponding efficiencies, Δt is the sample interval, and E_{nom} is nominal energy. This expression is included as a general modelling reference and is not asserted to be the exact equation used in the source project. The convention for positive power, the SOC scaling, and the model's efficiency treatment must be confirmed against the original Simulink implementation before the equation is used as a model-specific description.

Likewise, a practical controller should impose $SOC_{min} \leq SOC \leq SOC_{max}$ and bounds on charging/discharging power and converter current. For SMES, coil-current and converter constraints must be considered; for a supercapacitor, voltage and energy limits are relevant. If the reported results are to be interpreted as evidence of reduced battery stress, a useful extension would report battery RMS current, charge throughput, number and depth of SOC cycles, and an explicit degradation model. A narrower observed SOC interval is informative, but is not a substitute for these measures.

EDITOR-IN-CHIEF
Prof. Saeid Eslamian [IRAN]

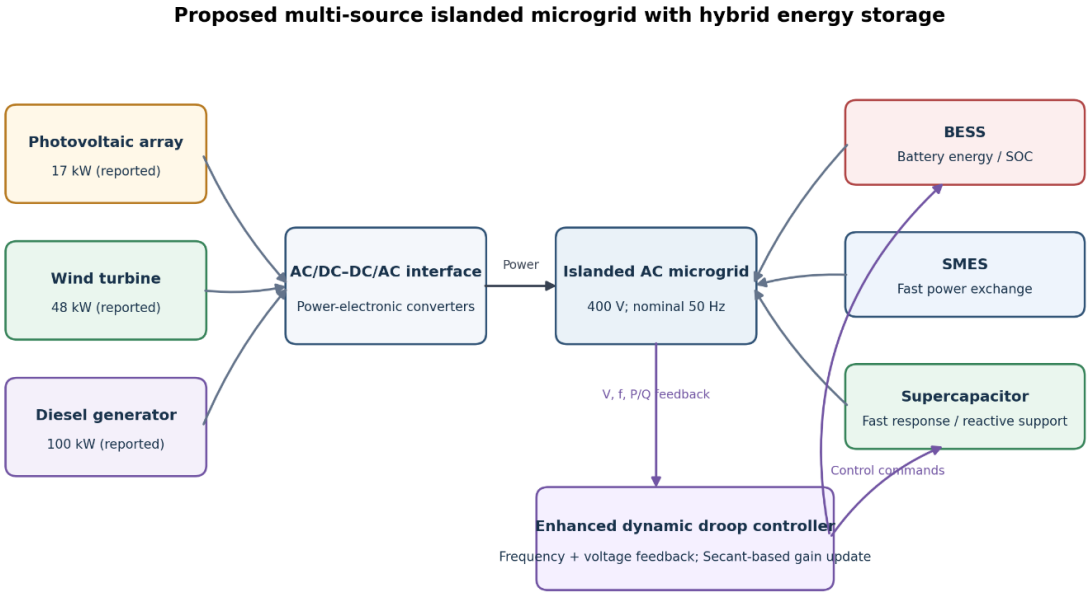

Figure 1. Conceptual architecture reconstructed from the project report. The drawing summarizes reported system components; it is not a reproduction of the original Simulink screenshot.

Storage components and reported parameters

Component	Reported parameter	Value
PV system	Rated power	17 kW
Wind turbine	Rated power	48 kW
Diesel generator	Rated power	100 kW
SMES	Inductance	1.4 H
SMES	Standard / critical current	150 A / 250 A
SMES	Energy capacity (as reported)	20.23 kJ
SMES	Highest power (as reported)	202.3 kW
BESS	Battery type / cell rating	Lead-acid, 60 Ah, 12 V
BESS	Matrix size	4 × 20
BESS	Power rating / maximum energy	10 kW / 100 kWh
Supercapacitor	Reactive power (as reported)	10 kVAr
Supercapacitor	Time constant	1×10^{-4} s

The parameter descriptions available in the source report require verification against the original model. In particular, the SMES energy and power ratings, the BESS bank terminal voltage, and the distinction between rated and maximum values are not sufficiently consistent or fully explained in the supplied text extract.

Control strategy

The controller measures microgrid frequency and voltage, compares them with nominal references, estimates active- and reactive-power deviations, and updates droop gains using prior

EDITOR-IN-CHIEF
Prof. Saeid Eslamian [IRAN]

measurements. The report describes the dynamic gain update as based on the conventional Secant method and contrasts it with constant droop gain. The resulting commands coordinate the storage devices subject to component operating limits. This approach is situated within established droop-based and hierarchical microgrid control [1], [2], [13], [14] and dynamic-droop control of a battery–SMES HESS in an isolated microgrid [12]. The exact update equations, gain limits, and claimed extension should be checked against the MATLAB code before publication.

Generic droop relationships and dynamic gain update

For a conventional droop-controlled inverter, simplified steady-state relationships are often written as Equs. 3&4

$$V_{mg} = V_{ref} + Droop_V \times (f_{mg} - f_{ref}) - Droop_{V_{BESS}} \times I_{BESS} - Droop_{V_{SMES}} \times I_{SMES} - Droop_{V_{SUPCA}} \times I_{SUPCA} \quad (3)$$

Where V_{mg} represents the microgrid voltage, V_{ref} is the voltage reference, $Droop_V$ is the voltage droop coefficient, f_{mg} is the microgrid frequency, f_{ref} is the frequency reference, $Droop_{V_{BESS}}$ is the voltage droop factor for battery, $Droop_{V_{SMES}}$ is voltage droop factor for SMES, $Droop_{V_{SUPCA}}$ represent voltage droop factor for supercapacitor, I_{BESS}, , is the currents flowing through the battery, I_{SMES} , is the currents flowing through the SMES, I_{SUPCA} , is the currents that flow in the supercapacitor

$$f_{MG} = f_{ref} + Droop_f \times (P_{MG} - P_{ref}) - Droop_{f_{BESS}} \times I_{BESS} - Droop_{f_{SMES}} \times I_{SMES} - Droop_{f_{SUPCA}} \times I_{SUPCA} \quad (4)$$

where: P_{MG} is the microgrid power, P_{ref} is the microgrid power reference, f_{MG} represents the microgrid frequency, f_{ref} is the frequency reference, $Droop_f$ is the frequency droop coefficient, $Droop_{f_{BESS}}$ represent frequency droop factor for battery, $Droop_{f_{SMES}}$ is frequency droop factor for SMES, $Droop_{f_{SUPCA}}$ represent frequency droop factor for supercapacitor, I_{BESS} represent currents that flow through the battery, I_{SMES} is the currents that flow through the SMES, I_{SUPCA} is the currents that flow through the SUPCA.

The Secant method is a numerical root-finding procedure that estimates a root using two prior function evaluations, commonly represented as Equ.5

$$x_{(k+1)} = x_k - f(x_k)\frac{x_k - x_{k-1}}{f(x_k) - f(x_{k-1})} \qquad \forall\, k \epsilon I \quad (5)$$

In a control application, the controlled quantity, objective function, update interval, initialization, denominator protection, gain saturation, and fallback behaviour must be defined before this equation can be mapped to a controller. A numerical root-finding formula alone does not establish closed-loop stability. The source report's description should therefore be checked against the

EDITOR-IN-CHIEF
Prof. Saeid Eslamian [IRAN]

actual MATLAB Function blocks or controller code to determine what variable is updated and how the Secant iteration is bounded.

For reproducibility, a complete controller specification should state the measured signals and filters; sampling and update rates; nominal references; initial gains; lower and upper gain limits; saturation and anti-windup logic; measurement-noise handling; storage dispatch priority; and the logic used when the Secant denominator approaches zero. It should also explain whether the controller is executed once per simulation step or iterated internally, and how it behaves when the operating point changes abruptly. These details matter because an adaptive gain can improve response under some conditions yet amplify noise or create excessive control action when updates are not bounded.

A fair comparison between constant and dynamic droop requires all other relevant conditions to be held constant: network and generation parameters, initial SOC, converter ratings, load disturbance, renewable profiles, simulation solver, sample time, and measurement windows. If these conditions differ between runs, the result cannot be attributed solely to the droop strategy. The available text extraction does not document all such settings, so they should be recovered from the original model before the study is submitted as a reproducible numerical comparison.

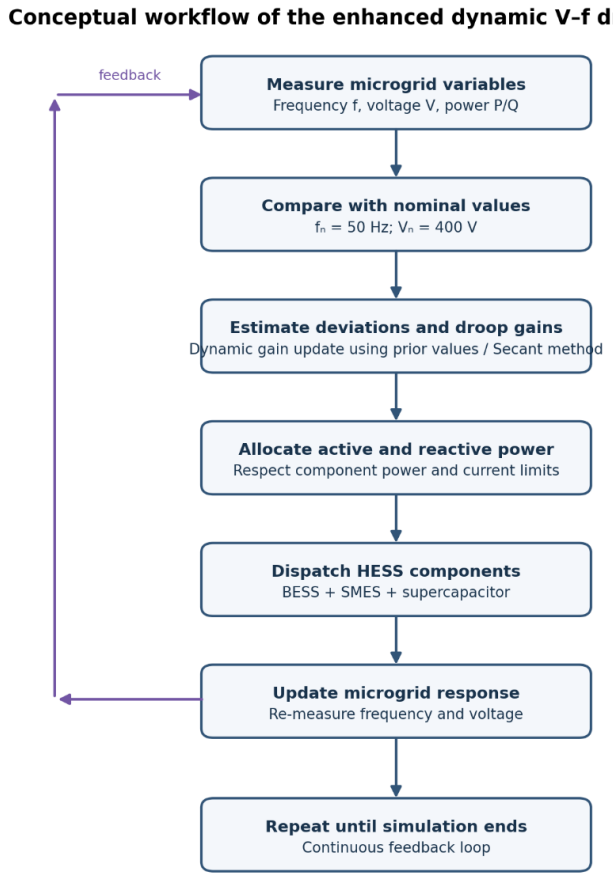

Figure 2. Conceptual feedback workflow of the enhanced dynamic voltage–frequency droop controller, reconstructed from the report's description and Appendix B.

EDITOR-IN-CHIEF
Prof. Saeid Eslamian [IRAN]

Simulation cases

The report compares the following configurations: (i) BESS only; (ii) BESS–SMES with constant droop gain; (iii) BESS–SMES with dynamic droop gain; (iv) BESS–SMES–supercapacitor with constant droop gain; and (v) BESS–SMES–supercapacitor with dynamic droop gain. The voltage and frequency comparison section also refers to a microgrid without storage, giving six operating conditions in total. The reported outputs include current, battery SOC, voltage deviation, frequency oscillation, and THD.

Performance indicators and comparison protocol

The available results permit direct comparison of the reported minimum and maximum battery SOC and the reported THD values. For each SOC interval, the width is calculated as $SOC_{max}-SOC_{min}$ in percentage points. This simple indicator is transparent and can be reproduced from the endpoints. It does not describe the time spent near the endpoints, the number of charge/discharge reversals, the battery current profile, or the amount of energy processed. Those quantities should be added if the original time series become available.

For frequency response, recommended quantitative indicators include maximum absolute frequency deviation, frequency nadir and zenith, settling time within a declared tolerance band, and the integral of absolute frequency error over a specified time horizon. Voltage performance can be assessed using maximum and minimum RMS voltage, peak deviation from nominal voltage, settling time, and an integral voltage-error metric. The disturbance type, magnitude, application time, recovery time, and tolerance band must be stated for each metric. Without these definitions, terms such as “faster,” “more stable,” or “better regulation” remain qualitative.

For power quality, the measured waveform must be identified explicitly—e.g., phase voltage, line voltage, or current—and the fundamental component and harmonic grouping method must be documented. The FFT window should contain an appropriate number of cycles, with sample rate, spectral resolution, windowing, and measurement duration stated. THD is generally defined as the root-sum-square of harmonic components divided by the fundamental component, expressed as a percentage. A reported value exceeding 100% can occur in particular distorted or low-fundamental conditions, but such a large result warrants checking whether the correct signal, fundamental bin, units, and scaling were used. The values here are therefore retained as reported values pending reanalysis, not certified compliance measurements [23], [24].

The minimum comparison protocol for a rerun should include one documented load step, one renewable-output disturbance, and one combined disturbance; identical initial conditions across cases; recorded active/reactive power and SOC for each storage device; and exported voltage/frequency time series. A sensitivity study should then vary at least one key uncertainty, such as load-step magnitude, renewable ramp rate, droop-gain limits, or initial SOC. These are proposed validation steps, not simulations claimed to have been performed in the source report.

Results and discussion

The following results are transcribed from the project report. They are simulation outputs as reported by the author; the present manuscript does not independently rerun the MATLAB/Simulink model.

EDITOR-IN-CHIEF
Prof. Saeid Eslamian [IRAN]

Configuration	Reported SOC range	Reported THD	Reported mean current
BESS only	5–92%	303.152%	6.1681 A
BESS + SMES, constant droop	25–82%	290.491%	5.7108 A
BESS + SMES, dynamic droop	28–80%	289.987%	6.3551 A
BESS + SMES + SC, constant droop	29–72%	287.973%	5.1625 A
BESS + SMES + SC, dynamic droop	48–74%	277.258%	6.4095 A

Battery state of charge

The reported SOC range is broadest for the BESS-only case (5–92%), indicating the largest charge-state excursions among the compared storage configurations. Adding SMES with constant droop narrows the reported range to 25–82%, while dynamic droop with BESS–SMES gives 28–80%. Adding the supercapacitor further narrows the range to 29–72% under constant droop. The narrowest reported span is 48–74% for the BESS–SMES–SC configuration with dynamic droop. This is a 26-percentage-point range, compared with 87 percentage points for BESS alone. Hybrid storage can redistribute fast and slower power demands across devices, but SOC range alone does not quantify cell degradation or establish longer service life; a validated degradation model and lifetime simulation are needed for that claim [9]–[12].

Quantitative comparison of SOC spans

Using the endpoints reported in the project, the SOC spans are 87 percentage points for BESS alone, 57 percentage points for BESS–SMES with constant droop, 52 percentage points for BESS–SMES with dynamic droop, 43 percentage points for BESS–SMES–SC with constant droop, and 26 percentage points for BESS–SMES–SC with dynamic droop. Relative to the BESS-only span, the reported span is lower by 30 percentage points for BESS–SMES constant droop, 35 percentage points for BESS–SMES dynamic droop, 44 percentage points for three-component HESS constant droop, and 61 percentage points for three-component HESS dynamic droop. Expressed as a relative reduction in span, these differences are approximately 34.5%, 40.2%, 50.6%, and 70.1%, respectively. These calculations use only the reported endpoints and should not be interpreted as reductions in battery degradation or energy throughput.

The comparison between the two BESS–SMES cases shows a 5-percentage-point reduction in SOC span when dynamic droop is used (57 to 52 percentage points). For the three-component arrangement, the dynamic-droop case has a 17-percentage-point narrower span than the constant-droop case (43 to 26 percentage points). This pattern is consistent with the hypothesis that adding a fast storage element and changing the gain schedule can alter the battery's response burden. However, because the SOC time series and dispatch signals are unavailable, the mechanism cannot be confirmed and other differences in the simulation setup cannot be excluded.

The reported minimum SOC of 48% in the BESS–SMES–SC dynamic-droop case is higher than the minimum in the other cases, but its maximum of 74% is not the highest. Thus, the narrowest interval

EDITOR-IN-CHIEF
Prof. Saeid Eslamian [IRAN]

reflects a different operating band as well as a smaller span. When comparing SOC management, both the width and the absolute endpoints matter: a narrow interval can still be inappropriate if it lies too close to a device's upper or lower limit, and an acceptable operating band depends on the battery chemistry, manufacturer limits, and chosen reserve policy.

Cross-case synthesis of storage and control effects

The five cases form a useful progression, but they do not constitute a complete factorial experiment. The BESS-only case differs in storage composition from all other cases; the BESS–SMES pair permits a comparison between constant and dynamic droop; and the three-component arrangement permits a second such comparison. This structure allows a descriptive comparison of the two droop modes within each hybrid arrangement, while the effect of adding a supercapacitor is assessed by comparing configurations that may differ in both device composition and controller mode. A formal attribution of improvement to one factor would require all combinations to be tested under the same initial conditions and disturbance profile.

For BESS–SMES, the SOC span changes from 57 percentage points under constant droop to 52 percentage points under dynamic droop, a reduction of 5 percentage points or approximately 8.8% relative to the constant-droop span. For BESS–SMES–SC, the span changes from 43 to 26 percentage points, a reduction of 17 percentage points or approximately 39.5%. The difference between these two reductions suggests that the apparent benefit associated with dynamic droop is not the same in the two reported storage arrangements. This is a descriptive observation, not a statistical or causal result, because the time series, repeat runs, and uncertainty estimates are unavailable.

The reported mean-current values also do not follow a simple monotonic pattern: 6.1681 A for BESS only, 5.7108 A for BESS–SMES constant droop, 6.3551 A for BESS–SMES dynamic droop, 5.1625 A for BESS–SMES–SC constant droop, and 6.4095 A for BESS–SMES–SC dynamic droop. The highest reported mean current is associated with the three-component dynamic-droop case, even though that case has the narrowest reported SOC interval. The current metric therefore needs a clear definition—what component and phase are measured, whether the value is signed or absolute, and whether it is a mean, RMS, or time-window statistic—before it can support a conclusion about reduced battery stress. This inconsistency is another reason not to infer battery-life extension from SOC endpoints alone.

A stronger comparative table would list, for every case, the storage composition, controller mode, SOC minimum, SOC maximum, SOC span, battery RMS current, cumulative absolute charge throughput, maximum frequency deviation, maximum voltage deviation, settling times, and validated THD. Each metric should be calculated from a declared interval and identical disturbances. If the raw model results cannot be recovered, the current manuscript should retain the reported SOC and THD values with explicit qualification and avoid filling the missing columns with estimates.

EDITOR-IN-CHIEF
Prof. Saeid Eslamian [IRAN]

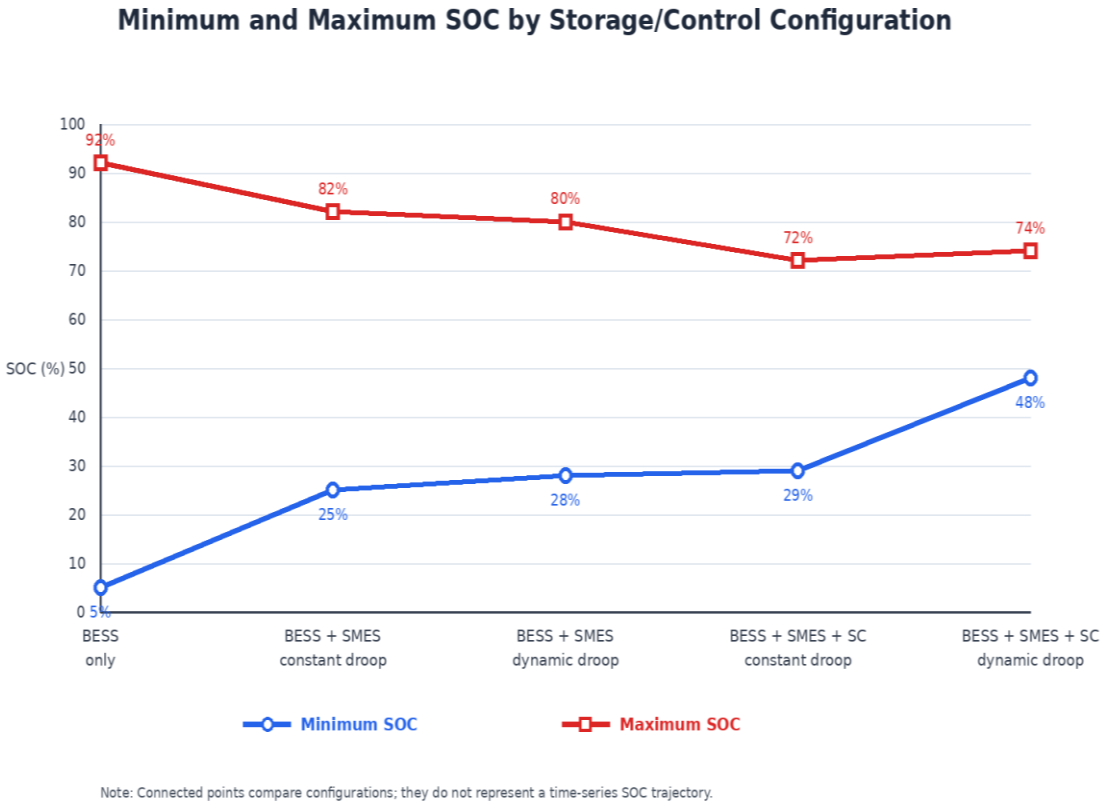

Figure 3. Reported battery SOC ranges for the five storage/control cases. Endpoints are taken from the report; intermediate trajectories are not reconstructed.

Harmonic distortion

The report gives THD values of 303.152% for BESS only, 290.491% for BESS–SMES with constant droop, 289.987% for BESS–SMES with dynamic droop, 287.973% for the three-component HESS with constant droop, and 277.258% for the three-component HESS with dynamic droop. The reported values decrease across the configurations, with the lowest value associated with the proposed HESS and DDG. However, these absolute values are unusually high for a regulated voltage waveform and cannot be accepted without validating the measurement procedure. Harmonic assessment should specify the measured signal, fundamental component, analysis window, sampling rate, and harmonic grouping, consistent with applicable power-quality measurement guidance such as IEC 61000-4-7 [23] and IEEE Std 519-2022 [24]. The trend is therefore reproduced as source-reported, not as independently validated power-quality performance.

Interpretation and verification of the reported THD ordering

The reported THD sequence decreases from 303.152% for BESS alone to 277.258% for the three-component HESS with dynamic droop. The absolute difference between these two reported values is 25.894 percentage points, equivalent to an approximately 8.54% relative reduction when calculated against the BESS-only value. The three-component dynamic-droop value is 10.715

EDITOR-IN-CHIEF
Prof. Saeid Eslamian [IRAN]

percentage points lower than the three-component constant-droop value. These arithmetic comparisons describe the reported numbers only; they do not establish that the waveforms meet a harmonic standard or that the THD measurement is correct.

A verification workflow should first identify the exact Simulink measurement block and signal tap used for each case. The fundamental component should be checked directly from the spectrum, and the THD calculation should be repeated using the same steady-state time window and sampling settings for all cases. The analyst should confirm whether the software reports voltage THD, current THD, or a distortion measure for another signal, and whether any percentage scaling or normalization is applied. If the fundamental component is very small relative to the harmonic components, a high THD ratio may be mathematically possible but may not be an informative measure of system power quality.

Only after this audit should the results be compared with the relevant limits. IEEE Std 519-2022 distinguishes voltage and current distortion considerations and depends on the applicable point of common coupling and system conditions; IEC 61000-4-7 provides measurement guidance for harmonics and interharmonics [23], [24]. A stand-alone microgrid simulation may not map directly to every grid-code limit. The manuscript should therefore report the measurement method and context first, then state any standard-based compliance conclusion only if the comparison is technically applicable.

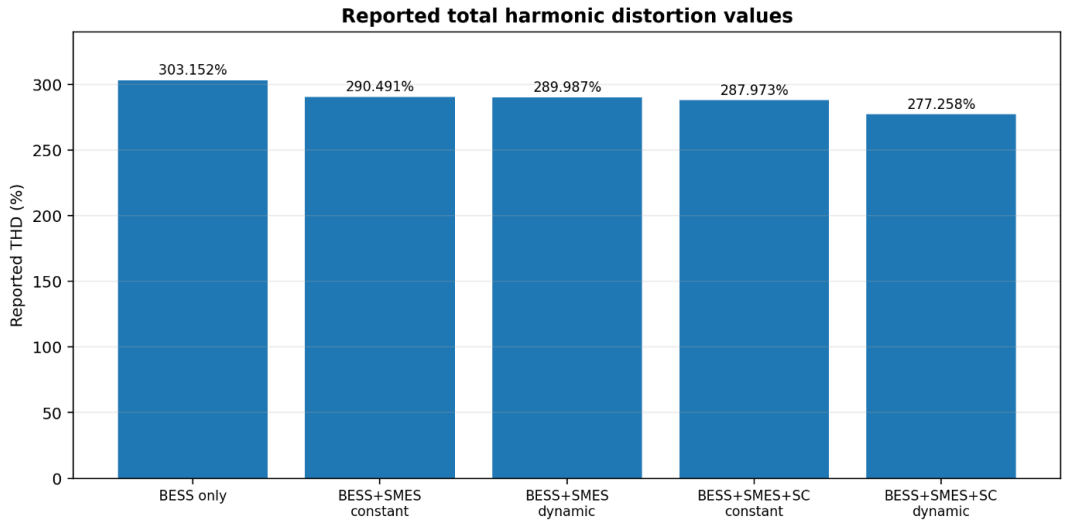

Figure 4. THD values as reported in the project report. The plot reproduces the reported numbers and does not validate the FFT calculation.

Voltage and frequency response

The report describes the no-storage microgrid as having the most severe voltage variations and frequency oscillations. HESS configurations are reported to reduce the amplitude of these excursions, and the BESS–SMES–supercapacitor arrangement with dynamic droop is identified as the best-performing case overall. The source text does not provide digitized time-series values, numerical peak deviations, settling times, or frequency nadir/zenith values. Therefore, this

manuscript does not fabricate response curves or claim a numerical improvement in voltage or frequency beyond the qualitative comparison documented in the report. For a journal submission, the original simulation data should be exported and plotted with clearly defined axes and disturbance timing.

Implications for controller and storage selection

The results illustrate why storage selection and controller selection should be considered jointly. A storage device changes the power and energy resources available to the controller, while the control law determines how those resources are called upon. The same dynamic gain schedule may therefore produce different outcomes when the system includes a battery alone, a battery with SMES, or a battery with both SMES and a supercapacitor. This interaction is a central motivation for hybrid storage, but it also means that a result from one configuration cannot be transferred automatically to another configuration or to a different microgrid.

A useful design decision should begin with the disturbance profile and service objective. If the dominant requirement is to bridge short, high-power transients, a fast storage device may be valuable even when its energy capacity is modest. If the requirement is to sustain a longer mismatch between generation and load, energy capacity and allowable duration become more important. If voltage regulation is the primary objective, the converter's reactive-power capability and network impedance may be as important as the storage technology. The design should therefore distinguish power rating, energy rating, response time, and control authority rather than treating the number of storage technologies as a direct measure of capability.

Dynamic droop can potentially adapt the trade-off between regulation and power sharing as operating conditions change. Its suitability, however, depends on bounded gain updates and a clear relationship between the measured error and the updated coefficient. An unbounded or poorly conditioned update can cause abrupt control action, amplify measurement noise, or interact adversely with converter limits. The Secant method is a numerical update mechanism; it does not independently guarantee closed-loop stability. A stability argument or a systematic robustness assessment is therefore needed before the controller is recommended for safety-critical operation.

On the evidence currently available, the most defensible selection statement is limited: the BESS–SMES–SC configuration with dynamic droop has the narrowest battery SOC interval among the five reported cases. That finding can motivate further testing of the arrangement, but it should not be treated as a complete selection rule. A final recommendation would require the verified frequency and voltage metrics, current and energy throughput, power-quality audit, device constraints, and lifecycle cost to be considered together. This multi-criteria view is consistent with the broader microgrid-control literature, which treats stability, sharing, energy management, and practical implementation as connected but distinct objectives [26]–[28].

What is needed for a quantitative dynamic comparison

A qualitative ranking of voltage and frequency traces is useful during exploratory modelling, but a journal comparison should present a common disturbance and metrics calculated from the same time series. For example, a frequency plot should identify the nominal 50 Hz reference, disturbance

EDITOR-IN-CHIEF
Prof. Saeid Eslamian [IRAN]

onset, pre-disturbance steady-state interval, and recovery interval. The associated table should report the maximum absolute deviation and the time required to return within a stated band. A voltage plot should state whether the reported 400 V is phase-to-phase RMS, peak, or another convention; otherwise the apparent deviation may be misinterpreted.

The no-storage case is an important baseline because it helps isolate the contribution of storage from the contribution of the generation mix and primary controller. It should be included in the same results table as the five storage/control configurations if it was simulated under comparable conditions. Since the project text alternates between five and six operating conditions, the exact case count and naming should be reconciled with the original figures and model. A table of cases should record storage devices, droop mode, initial SOC, disturbance, and any controller changes, so that comparisons are traceable.

Transient response can also depend on the diesel generator governor and exciter, the PV and wind converter controls, filter parameters, line impedance, and the load model. Consequently, an observed improvement should not be attributed to the HESS alone unless these other elements are held fixed. If the model includes current limiting or protection logic, the event logs should be checked for limit activation because saturation can materially change the shape of a response. The source extract does not include these details, so they are identified here as requirements for a strengthened rerun rather than as facts about the existing simulations.

Limitations and reproducibility considerations

Several limitations should be addressed before submission. First, the supplied source is a text extraction of the project report; the original embedded Simulink diagrams and result plots were not available as image files, so the architecture and control workflow figures in this manuscript are conceptual redrawing's. Second, the report's numerical time-series data and simulation files are not included, preventing independent reproduction of the response curves. Third, the reported THD values and fundamental-frequency/FFT details need verification. Fourth, the source report notes that the control approach may not perform adequately during transitions between grid-connected and islanded operation, and that residual harmonic currents remain. Fifth, the source report's case descriptions are inconsistent: one section describes five storage/control cases, while the voltage/frequency section also includes a no-storage case. Finally, component parameters, controller implementation, and the bibliography should be checked against the original model and publications. The paper should not claim a numerical improvement in battery lifetime unless a lifetime/degradation model was actually run.

Recommended reproducibility checklist

Before final submission, the model should be audited against a compact reproducibility checklist. The system-level record should include a single-line diagram, bus voltage convention, nominal frequency, line and transformer parameters, load model, generation ratings, renewable profiles, diesel governor/exciter parameters, and converter switching or averaged-model assumptions. The storage record should specify usable energy, rated power, current/voltage limits, efficiency, SOC limits, initial conditions, and any thermal or protection constraints. The controller record should

EDITOR-IN-CHIEF
Prof. Saeid Eslamian [IRAN]

include equations, units, sample times, gain initialization and bounds, filter constants, saturation logic, and the mapping from measured errors to device commands.

The numerical study should report the solver, integration step, simulation duration, controller sampling time, initial steady-state conditions, and disturbance timing. Each comparison should be rerun from the same initial state or the differences should be explicitly justified. Raw data should be exported in a machine-readable format, and figure generation should be reproducible from scripts. At minimum, the data package should contain voltage, frequency, active and reactive power, battery SOC/current, SMES current or energy, supercapacitor voltage or energy, and the THD calculation settings. These records would allow another researcher to verify the ranking reported in the paper.

A sensitivity analysis should examine whether the reported ranking persists under plausible parameter variation. Candidate factors include initial battery SOC, load level and step size, PV irradiance ramps, wind-speed changes, storage power limits, droop coefficients, and controller sample time. Results should be reported for both nominal and stressed conditions. If computational resources are limited, a small, clearly defined one-factor-at-a-time study is preferable to a broad but undocumented claim of robustness. No robustness claim should be made until such a study has been completed.

Threats to validity and interpretation

The principal threat to internal validity is that the source report does not provide enough detail to determine whether all cases used identical disturbance profiles, initial conditions, and measurement windows. The principal threat to measurement validity is the unusually large reported THD, which requires rechecking before any power-quality claim can be accepted. The principal threat to construct validity is treating SOC range as a proxy for battery lifetime: the interval is a useful indicator of SOC excursion, but lifetime also depends on current, temperature, depth of discharge, cycling frequency, calendar ageing, and cell chemistry. These distinctions are important to avoid over claiming from the available evidence.

A further threat is external validity. A simulated PV–wind–diesel microgrid with the reported ratings does not by itself establish performance in other microgrid sizes, network impedances, storage technologies, or operating environments. Practical SMES deployment in particular may introduce cost, cryogenic, and protection constraints that are not represented by a simplified simulation. Similarly, an adaptive controller's behaviour can change under sensor noise, communication delay, converter saturation, and islanding transitions. These limitations do not invalidate the project as a comparative simulation, but they define the scope of the conclusions that can reasonably be drawn.

Future work

The most immediate next step is to recover the original Simulink model and verify every reported parameter and output. The second is to reconstruct the controller equations from the implementation and compare them directly with the earlier dynamic-droop method. The third is to rerun the cases with identical disturbances and report standardised voltage, frequency, SOC, and power-quality metrics. The fourth is to add an explicit battery ageing model and compare

EDITOR-IN-CHIEF
Prof. Saeid Eslamian [IRAN]

cumulative degradation under matched duty cycles. Finally, a robustness study and, where feasible, controller-hardware or real-time simulation would strengthen the evidence for practical applicability. These are proposed extensions and should not be described as completed work.

Practical implementation considerations

The practical value of a multi-technology HESS depends on more than the dynamic response observed in a simulation. A battery-based unit requires a battery-management system, cell balancing, temperature monitoring, and protection against overcurrent, overvoltage, under voltage, and unacceptable SOC. A supercapacitor unit requires a converter and control that keep its terminal voltage within an admissible window; because stored energy is proportional to the square of voltage, the available energy changes nonlinearly with terminal voltage. A SMES unit requires superconducting coil protection and a thermal/cryogenic subsystem in addition to its converter. These auxiliary systems influence cost, efficiency, maintenance, and availability, and should be acknowledged when the configuration is discussed as a candidate for real islanded microgrids.

Coordination should also be designed to prevent simultaneous saturation of multiple storage devices. If the battery reaches its power or SOC limit during a disturbance, the remaining devices must have sufficient headroom to contribute; otherwise the nominal HESS may behave much like a single constrained storage unit. Conversely, if the fast devices are dispatched for sustained energy imbalance, they may exhaust their usable energy or reach current/voltage limits before the event has passed. A supervisory layer can help allocate low-frequency energy demand to the battery and high-frequency transients to fast devices, but the present report does not provide enough detail to determine whether such explicit frequency separation or dispatch logic was implemented.

Islanded microgrids also experience operating-mode changes and communication or sensor imperfections. A controller tuned for steady islanded operation may behave differently during start-up, reconnection, loss of a generation source, or transition into current limiting. For this reason, a practical assessment should include protection coordination and transitions, not just a nominal load disturbance. The source project itself notes limitations around transitions and residual harmonic currents; these observations should remain visible in the final interpretation rather than being obscured by the ranking of the five reported cases.

Economic feasibility is outside the numerical evidence currently available. A fair system-level comparison would consider capital cost, round-trip efficiency, auxiliary power consumption, expected service life, replacement intervals, and the cost of SMES cryogenic infrastructure. A configuration that improves a selected dynamic metric may not be the lowest-cost or most maintainable option. Future work could compare the cost per unit of frequency-support capability or the lifecycle cost under a specified disturbance profile, provided that reliable device cost and lifetime assumptions are documented.

Conclusion

This study investigated a multi-source islanded microgrid supported by a hybrid energy storage system comprising BESS, SMES, and a supercapacitor, controlled using an enhanced dynamic

EDITOR-IN-CHIEF
Prof. Saeid Eslamian [IRAN]

droop strategy. According to the project's MATLAB/Simulink results, the three-component HESS with dynamic droop produced the narrowest reported battery SOC range (48–74%) and the lowest reported THD (277.258%) among the compared storage/control cases. The report also qualitatively identifies improved voltage and frequency regulation relative to configurations with less storage support or fixed droop gains. The proposed combination is therefore a promising control concept for coordinating fast and energy-dense storage technologies. Further validation requires release of simulation time series, confirmation of component parameters, rechecking of the THD calculation, and quantitative reporting of frequency nadir, voltage deviation, settling time, and battery degradation or lifetime.

The clearest quantitative finding available from the source report is the ordering of battery SOC spans across the five storage/control cases. The span narrows from 87 percentage points for BESS alone to 26 percentage points for the BESS–SMES–SC arrangement with dynamic droop. The reported THD values also follow a decreasing order, but their unusually high absolute magnitude and undocumented FFT settings prevent a defensible compliance conclusion. Voltage and frequency responses are described qualitatively only because numerical trajectories and metrics were not available in the supplied extract.

Accordingly, the results support a cautious conclusion that the three-component hybrid arrangement with dynamic droop is associated with the narrowest reported battery SOC interval in the project's comparison. They do not, on their own, establish longer battery life, verified harmonic compliance, a quantified improvement in frequency nadir or voltage deviation, or general superiority across operating conditions. The strongest next contribution would be a reproducible rerun that reports raw time series, transparent control equations, and matched quantitative comparisons, while explicitly disclosing the relationship to the author's related prior publication.

References

[1] E. Barklund, N. Pogaku, M. Prodanovic, C. Hernandez-Aramburo, and T. C. Green, "Energy management in autonomous microgrid using stability-constrained droop control of inverters," IEEE Transactions on Power Electronics, vol. 23, no. 5, pp. 2346–2352, 2008. doi: 10.1109/TPEL.2008.2001910.

[2] J. M. Guerrero, J. C. Vásquez, J. Matas, L. G. de Vicuña, and M. Castilla, "Hierarchical control of droop-controlled AC and DC microgrids—A general approach toward standardization," IEEE Transactions on Industrial Electronics, vol. 58, no. 1, pp. 158–172, 2011. doi: 10.1109/TIE.2010.2066534.

[3] H. Bevrani, A. Ghosh, and G. Ledwich, "Renewable energy sources and frequency regulation: Survey and new perspectives," IET Renewable Power Generation, vol. 4, no. 5, pp. 438–457, 2010.

[4] G. Delille, B. François, and G. Malarange, "Dynamic frequency control support by energy storage to reduce the impact of wind and solar generation on isolated power system's inertia," IEEE Transactions on Sustainable Energy, vol. 3, no. 4, pp. 931–939, 2012. doi: 10.1109/TSTE.2012.2205025.

[5] D. E. Olivares et al., "Trends in microgrid control," IEEE Transactions on Smart Grid, vol. 5, no. 4, pp. 1905–1919, 2014. doi: 10.1109/TSG.2013.2295514.

[6] H. Chen, T. N. Cong, W. Yang, C. Tan, Y. Li, and Y. Ding, "Progress in electrical energy storage system: A critical review," Progress in Natural Science, vol. 19, no. 3, pp. 291–312, 2009. doi: 10.1016/j.pnsc.2008.07.014.

[7] X. Luo, J. Wang, M. Dooner, and J. Clarke, "Overview of current development in electrical energy storage technologies and the application potential in power system operation," Applied Energy, vol. 137, pp. 511–536, 2015.

[8] S. Hajiaghasi, A. Salemnia, and M. Hamzeh, "Hybrid energy storage system for microgrids applications: A review," Journal of Energy Storage, vol. 21, pp. 543–570, 2019. doi: 10.1016/j.est.2018.12.017.

EDITOR-IN-CHIEF
Prof. Saeid Eslamian [IRAN]

[9] W. Jing, C. H. Lai, S. H. W. Wong, and M. L. D. Wong, "Battery-supercapacitor hybrid energy storage system in standalone DC microgrids: A review," IET Renewable Power Generation, vol. 11, no. 4, pp. 461–469, 2017. doi: 10.1049/iet-rpg.2016.0500.

[10] M. Khalid, "A review on the selected applications of battery-supercapacitor hybrid energy storage systems for microgrids," Energies, vol. 12, no. 23, Art. no. 4559, 2019. doi: 10.3390/en12234559.

[11] J. Li, A. M. Gee, M. Zhang, and W. Yuan, "Analysis of battery lifetime extension in a SMES-battery hybrid energy storage system using a novel battery lifetime model," Energy, vol. 86, pp. 175–185, 2015. doi: 10.1016/j.energy.2015.03.132.

[12] J. Li, R. Xiong, Q. Yang, F. Liang, M. Zhang, and W. Yuan, "Design/test of a hybrid energy storage system for primary frequency control using a dynamic droop method in an isolated microgrid power system," Applied Energy, vol. 201, pp. 257–269, 2017. doi: 10.1016/j.apenergy.2016.10.066.

[13] K. De Brabandere, B. Bolsens, J. Van den Keybus, A. Woyte, J. Driesen, and R. Belmans, "A voltage and frequency droop control method for parallel inverters," IEEE Transactions on Power Electronics, vol. 22, no. 4, pp. 1107–1115, 2007.

[14] J. Rocabert, A. Luna, F. Blaabjerg, and P. Rodríguez, "Control of power converters in AC microgrids," IEEE Transactions on Power Electronics, vol. 27, no. 11, pp. 4734–4749, 2012. doi: 10.1109/TPEL.2012.2199334.

[15] A. González, E. Goikolea, J. A. Barrena, and R. Mysyk, "Review on supercapacitors: Technologies and materials," Renewable and Sustainable Energy Reviews, vol. 58, pp. 1189–1206, 2016.

[16] X. Lin and R. Zamora, "Controls of hybrid energy storage systems in microgrids: Critical review, case study and future trends," Journal of Energy Storage, vol. 45, Art. no. 103884, 2022. doi: 10.1016/j.est.2021.103884.

[17] P. Mercier, R. Cherkaoui, and A. Oudalov, "Optimizing a battery energy storage system for frequency control application in an isolated power system," IEEE Transactions on Power Systems, vol. 24, no. 3, pp. 1469–1477, 2009.

[18] M. Aghamohammadi and H. Abdolahinia, "A new approach for optimal sizing of battery energy storage system for primary frequency control of islanded microgrid," International Journal of Electrical Power & Energy Systems, vol. 54, pp. 325–333, 2014. doi: 10.1016/j.ijepes.2013.07.005.

[19] I. Serban and C. Marinescu, "Control strategy of three-phase battery energy storage systems for frequency support in microgrids and with uninterrupted supply of local loads," IEEE Transactions on Power Electronics, vol. 29, no. 9, pp. 5010–5020, 2014.

[20] F. Díaz-González, M. Hau, A. Sumper, and O. Gomis-Bellmunt, "Participation of wind power plants in system frequency control: Review of grid code requirements and control methods," Renewable and Sustainable Energy Reviews, vol. 34, pp. 551–564, 2014.

[21] A. Ulbig, T. S. Borsche, and G. Andersson, "Impact of low rotational inertia on power system stability and operation," IFAC Proceedings Volumes, vol. 47, no. 3, pp. 7290–7297, 2014.

[22] T. Ma, H. Yang, and L. Lu, "A feasibility study of a stand-alone hybrid solar–wind–battery system for a remote island," Applied Energy, vol. 121, pp. 149–158, 2014.

[23] International Electrotechnical Commission, Electromagnetic compatibility (EMC)—Part 4-7: Testing and measurement techniques—General guide on harmonics and interharmonics measurements and instrumentation, for power supply systems and equipment connected thereto, IEC 61000-4-7, 2002.

[24] IEEE, IEEE Standard 519-2022: IEEE Standard for Harmonic Control in Electric Power Systems, 2022.

[25] C. Nayar, M. Tang, and W. Suponthana, "Wind/PV/diesel micro grid system implemented in remote islands in the Republic of Maldives," in Proceedings of the IEEE International Conference on Sustainable Energy Technologies, 2008, pp. 1076–1080.

[26] E. Planas, A. Gil-de-Muro, J. Andreu, I. Kortabarria, and I. Martínez de Alegría, "General aspects, hierarchical controls and droop methods in microgrids: A review," Renewable and Sustainable Energy Reviews, vol. 17, pp. 147–159, 2013. doi: 10.1016/j.rser.2012.09.032.

[27] K. N. Yogithanjali Saimadhuri and M. Janaki, "Advanced control strategies for microgrids: A review of droop control and virtual impedance techniques," Results in Engineering, vol. 25, Art. no. 103799, 2025. doi: 10.1016/j.rineng.2024.103799.

[28] G. Shahgholian, M. Moradian, and A. Fathollahi, "Droop control strategy in inverter-based microgrids: A brief review on analysis and application in islanded mode of operation," IET Renewable Power Generation, vol. 19, no. 1, Art. no. e13186, 2025. doi: 10.1049/rpg2.13186.

EDITOR-IN-CHIEF
Prof. Saeid Eslamian [IRAN]